Renewable Energy 160 (2020) 987–997

Contents lists available at ScienceDirect

Renewable Energy

journal homepage: www.elsevier.com/locate/renene

Probabilistic failure rate model of a tidal turbine pitch system

Fraser J. Ewing [a, *], Philipp R. Thies [b], Jonathan Shek [c], Claudio Bittencourt Ferreira [d]

[a] Industrial Doctoral Centre for Offshore Renewable Energy, University of Edinburgh, UK
[b] College of Engineering, Mathematics and Physical Sciences, University of Exeter, UK
[c] School of Engineering, University of Edinburgh, UK
[d] Renewables Certification, DNV GL, UK

ARTICLE INFO

Article history:
Received 26 June 2019
Received in revised form
6 June 2020
Accepted 29 June 2020
Available online 19 July 2020

Keywords:
Tidal turbine
Reliability prediction
Pitch system
Physics of failure
Failure rate

ABSTRACT

Accurate reliability prediction for tidal turbines is challenging due to scarce reliability data. To achieve commercialization, it is widely acknowledged that reductions in maintenance costs are vital and robust component reliability assessments can help drive this. For established technologies, reliability prediction either involves a statistical assessment of historical failure data, or a physics of failure approach based on dedicated accelerated testing. However, for low/mid Technology Readiness Level tidal developers these common approaches are difficult. Thus, developers require a method of making reliability predictions for components in the absence of tidal turbine specific failure data and physical testing results. This paper presents a failure rate model for a tidal turbine pitch system using empirical Physics of Failure equations, with associated uncertainties. Critical component design parameters are determined and their effects on the failure rate investigated via a sensitivity analysis. The modelled failure rate is then compared with wind turbine failure data from a series of turbines. The tidal turbine failure rate is approximately 50% lower, however high reliability requirements mean this is unlikely to be acceptable. The developed model can assist turbine developers in estimating failure rates and determining reliability critical design parameters for the failure critical pitch system.

1. Introduction

Accurate reliability prediction for a component or device is a challenging task. Component reliability is affected by several factors including the design, operating profile and environmental conditions. It is vital for tidal turbine developers to make reliability predictions in order to understand the reliability of their designs (enabling iterative design improvement) and hence the potential future maintenance strategies for their turbine deployments. Reliability of turbine components is widely acknowledged by the industry as being a critical driver of the cost of energy [1]. Attracting investment also relies heavily on being able to demonstrate high device availability and reliability [2]. During the design stage, particularly for new technologies such as tidal turbines, it is notoriously difficult to assess component reliability due to the inherent lack of operational or historical data to inform predictions. Ideally, detailed Accelerated Life Test (ALT) programs would be carried out for all failure critical components and these would form the basis of reliability predictions [1]. However, the costly nature of such activities mean that often developers in the low/mid Technology Readiness Level (TRL) stages may only have limited information such as basic component design parameters on which to base their reliability predictions. This presents an issue for tidal turbine developers: how can component reliability predictions be made without a dedicated accelerated testing regime and without operational failure data?

Tidal turbine component reliability studies often struggle with a lack of published data as well as commercial sensitivities. In Ref. [3], Val & Chernin estimate failure rate distributions of mechanical components (main bearing and seal) using empirical Physics of Failure equations and then update the failure rate distributions via a Bayesian update where the likelihood function is a Poisson Distribution of hypothetical failure events. The effect of the failure events on the failure rate distribution is demonstrated. In Ref. [4], Delorm uses historical failure data from surrogate industries (OREDA, WindStats and the LWK database) and uses the parts count reliability prediction method developed by the US Military in

* Corresponding author.
E-mail addresses: f.ewing@ed.ac.uk (F.J. Ewing), p.r.thies@exeter.ac.uk (P.R. Thies), j.shek@ed.ac.uk (J. Shek), claudio.bittencourt.ferreira@dnvgl.com (C.B. Ferreira).

https://doi.org/10.1016/j.renene.2020.06.142

Ref. [5] to assess the high-level designs of five notional tidal turbine architectures. In Ref. [6] Thies et al. develop a Bayesian method to assess the uncertainty around the failure rate of a notional wave energy converter umbilical cable. Failure data from the OREDA handbook is used as prior information and a Weibull distribution of the component failure rate (using hypothetical parameters to represent two failure scenarios) is constructed. The Bayesian method is utilized to show how the uncertainty around the reliability model parameters can be quantified. These prominent studies have tended to focus on methods to quantify uncertainties in component failure rates. The approach presented in this paper builds on this previous work by developing a complete component failure rate model with quantified uncertainties; importantly the effects of the critical design parameters on the overall reliability are investigated.

Pitch systems are used on the majority of modern horizontal axis turbines. Despite adding complexity via extra moving parts, they are attractive as a design choice because they maximize energy capture from the tidal flow (and also reduce blade bending moments). Experiences from the wind industry have shown that pitch systems are particularly prone to failure [7]. Although representing a small fraction of the total turbine cost [8], pitch systems can have a significant impact on overall reliability. Studies have shown that 30% of turbine failures can be attributed to them [9].

This paper presents a physics-based reliability prediction framework to make probabilistic failure rate estimations for the failure critical pitch system. The effects of design changes on the failure rate distribution are explored. The significance of this for tidal developers is that they can make component reliability predictions using only basic design parameters. Section 2 provides the theoretical background for the paper with a focus on reliability theory, failure rate modelling and physics of failure equations. Section 3 outlines the method for the development of the pitch system failure rate model. Section 4 presents the results of the model and compares the key findings with similarly rated wind turbines. Section 5 performs a sensitivity study and demonstrates the effects of variations in the critical design parameters. The paper concludes with a discussion in section 6, placing the results in the context of wider research and outlining limitations of the model.

2. Theoretical background

Reliability is a probabilistic measure of the ability of a component/system to perform its stated function for a required amount of time [10]. One of the critical drivers of reliability is the design of the component [11]. A poorly specified or incorrect design can result in the component not being fit for the purpose intended. For a nascent industry such as tidal energy it is not uncommon for developers to use 'off the shelf' components from more developed technologies such as wind turbines. Therefore, the components may not have been specifically designed for use in the subsea environment. This makes design stage reliability assessments crucial.

Another critical driver of reliability is uncertainty around the loading conditions of the component [12]. This is particularly relevant in the tidal sector where quantification of the tidal resource is associated with considerable uncertainty [13]. This uncertainty can then propagate into the turbine design via large safety factors, which adds to the cost of development of the turbine.

2.1. Failure rate modelling

Failure rate modelling is key for reliability prediction at the design stage. The objectives of reliability prediction include: the need to establish a baseline for logistic support requirements (e.g. maintenance); the need to improve or assess a design; the need to determine if a reliability objective is achievable [14]. There are several methods which are typically categorized as either statistical or physical. Statistical methods of reliability prediction focus on the use of applicable historical failure data to make inferences and predictions about the components lifetime. The failure data may come from the field or the laboratory. Given the nascent stage of the tidal energy industry, there is scant historical failure data publicly available so statistical approaches are not currently applicable.

Physical (or physics based) methods of reliability prediction involve Physics of Failure equations that are either empirically determined using Accelerated Life Test data or, where possible, fundamental laws of physics. Physics of Failure modelling requires detailed understanding of the electrical, mechanical and chemical stresses and material properties of a component [15]. The empirical Physics of Failure models used in this research are from Refs. [16]. The equations were developed specifically for the design evaluation of mechanical parts. Critical design parameters, environmental extremes and operational stresses are all incorporated within the equations which were developed using laboratory based Accelerated Life Test procedures. The equations correct a base failure rate for a component using influence factors that have been empirically derived based on physical principles and material properties. The influence factors must be determined for each component using design parameters. The influence factors are typically deterministic, however to reflect their uncertainty the most important factors are represented probabilistically using the Generalized Lognormal distribution (GLN). The level of uncertainty associated with each influence factor distribution is directly specified using the Coefficient of Variation (COV). The design parameters are calculated in Section 3 for the notional turbine design outlined in Section 2.2.

The GLN is commonly used in failure data analysis as it is positively skewed, which results in conservatively high component failure rate estimations. The GLN is used in the demonstrated approach to represent component failure rates. The GLN probability density function (PDF) is typically represented in the following format:

$$f\left(C_x,\theta,\sigma,m\right)=\frac{1}{\left(\lambda-\theta\right)\sigma\sqrt{2\pi}}exp\left(\frac{-log^2\left(\frac{C_x-\theta}{m}\right)}{2\sigma^2}\right) \quad (1)$$

where C_x represents a component design parameter, θ is the location parameter which represents the minimum threshold for the distribution (this is generally set to near zero), σ is the shape parameter which is equal to the COV for the GLN. m is the scale parameter which is used to define the center point (expected value) of the distribution. Representing component design parameters as GLN distributions means that the overall failure rate of the component is also represented by a GLN, thanks to the Central Limit Theorem.

2.2. Tidal turbine pitch system design

The notional horizontal axis tidal turbine in this work (highlighted in Fig. 1) is based on a typical pre-commercial design [17]. It has a rating of 1.5 MW at 3 m/s flow speed and has an 18 m diameter rotor. It is seabed mounted and typically deployed in tidal sites with a mean sea depth of 40–50 m.

The pitch system unit (highlighted in Fig. 2) is housed in the hub at the front of the turbine. It operates at rated flow speed to feather the blades and shed load to maintain rated electrical power output. It is electro-mechanical which is a common design choice and has been used extensively in the wind industry. In recent years, there has been a trend away from hydraulic pitch systems which

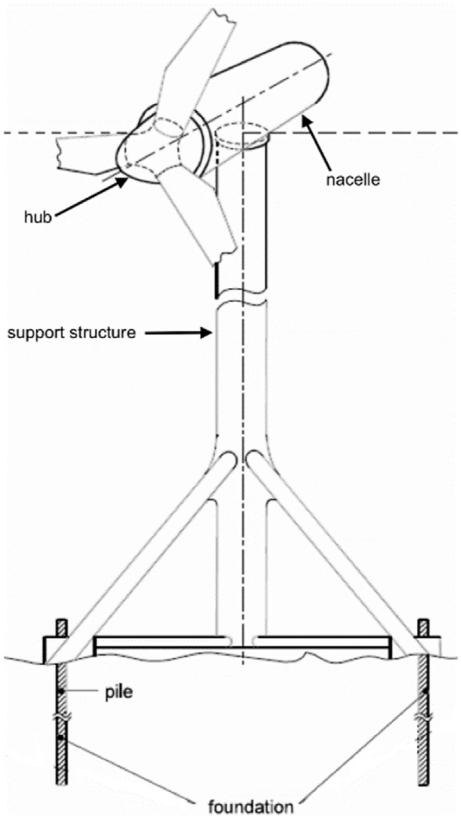

Fig. 1. Diagram of a horizontal axis tidal turbine. Reproduced with permission from DNV GL-ST-0164, Copyright DNV GL 2015 [18].

traditionally have been more unreliable than electro-mechanical ones [19].

An electro-mechanical pitch system typically consists of a voltage source (e.g. a battery or capacitor); pitch motor; brake; gearbox (with a pinion gear interacting with each blade); hub frame; and a roller bearing and dynamic seal at each blade interface. The overall design is a consequence of several factors. The design philosophy of the entire turbine feeds into the specifics of the pitch system design. Designing a turbine for a high overall reliability may mean reducing the number of moving parts and components which can come at the expense of power production. Space and weight requirements in the nacelle hub also impact the specifics of the pitch system design. The

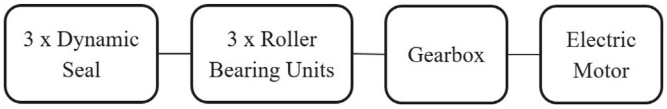

Fig. 3. Reliability Block Diagram for the electro-mechanical pitch system unit.

layout of the electrical circuitry, type of power take off/generating system and servicing/maintenance requirements also have a major influence on the pitch system design. The tidal industry, unlike the wind industry, is still very much in the turbine development stage of industrial development and thus the design choices for the turbine layout and component selection are numerous. It is for this reason that it is important for tidal developers to understand the reliability influencing factors of component design choices in order to make informed design decisions. The critical influencing factors for the pitch system are demonstrated in the Sensitivity Analysis in Section 5.

2.2.1. Reliability Block Diagram

The notional turbine in this work is designed with a focus on high component reliability. Developers currently at the forefront of the Tidal industry (e.g. SIMEC Atlantis, Nova Innovation, Orbital Marine Power) all prominently mention turbine reliability as a key design driver in their publications and websites [21–23]. The pitch system design for the notional turbine tries to minimize the number of components. Therefore, it has one drive unit which results in a collective pitching of the blades – rather than independent pitching which is common in the wind industry. The drive unit consists of a DC motor and small gearbox. The notional pitch system also consists of a dynamic seal and roller bearing unit at the interface of each blade. A Reliability Block Diagram (RBD) for the system can be seen in Fig. 3. These components represent the major parts of the pitch system (other components such as the hub frame and brake are not included). The design detail for each component is discussed in Section 2.2.3.

Fig. 3 represents a series configuration where all the components are failure critical; any component failure results in the stoppage of the turbine. The RBD for this series system of components is calculated as:

$$R_{system} = \prod_{i=1}^{n} R_i = \prod_{i=1}^{n} e^{-\lambda_i t} \tag{2}$$

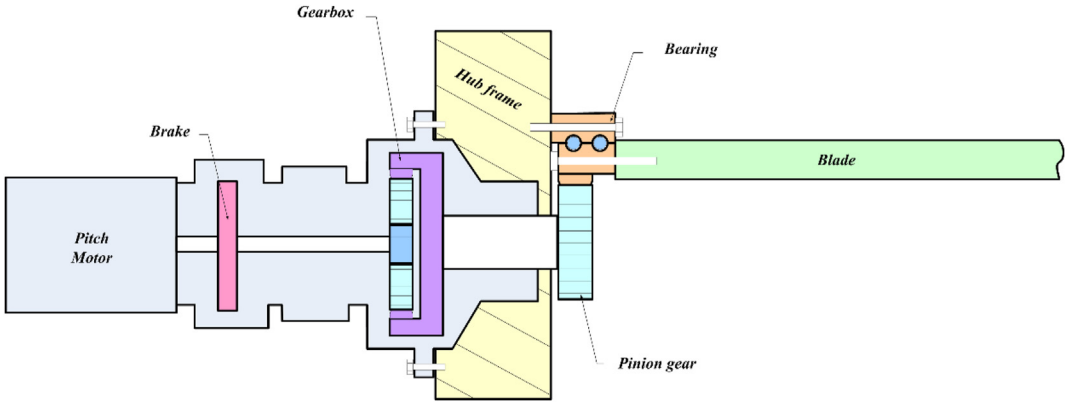

Fig. 2. Diagram of an electro-mechanical pitch system. Reproduced with permission from EWEC 2010: Scientific Proceedings European Wind Energy Conference & Exhibition, J. G. Holierhoek et al., "Setting up a prototype measurement campaign for mechanical components", Copyright WindEurope 2010 [20].

where the total system reliability R_{system} is the product of the i series component reliabilities. Each components reliability function R_i is represented via an exponential distribution which imposes an assumption of random, independent failures governed by the failure rate λ_i.

2.2.2. Operating profile

The operating profile of a tidal turbine pitch system depends on the operating regime of the turbine. The turbine design philosophy along with a detailed understanding of the specifics of the flow regime of the potential site will dictate the overall rating of the turbine. Typically, the pitch system will only operate at rated power, therefore the choice of turbine rating dictates how often the pitch system operates. Maximizing generation via a high turbine rating means increased power production but also increased capital expenditure on larger components. In this research a rating of 3 m/s is selected and it is assumed that the tidal regime at the proposed turbine site spends approximately 2 h every tidal cycle at or above this flow speed. This results in the pitch system operating for approximately 33% of every tide (which for a semidiurnal regime in the North of Scotland is approximately 6.25 h per tide [24]).

2.2.3. Component design details

The bearing unit for the pitch system is a single row thrust tapered unit. The bearings are thrust bearings as the principal load is an eccentrically applied thrust resulting in axial and overturning moment loads. Roller bearings preferred to ball bearings as they can accommodate heavier loads and lower speeds, which makes them well suited for tidal turbine applications. The design used here is based on the SKF BT1-8010 [25]. The mass of each bearing unit is 265 kg with a dynamic load rating of 3190 kN.

Dynamic seals are employed to prevent water ingress at each blade interface. The dynamic seal is designed specifically for tidal turbine applications and is based on the Wärtsilä OFS3H–N [26]. The seal diameter (D) is dependent on the diameter of the root of the turbine blade which for a 9-m blade can reasonably be assumed as 560 mm (22 inches).

The electric motor is powered either by battery or the grid supply and interfaces with the gearbox system. Electric motor reliability is determined by the reliability of the individual parts of the machine. The parts can include bearings, windings, armature, housing, brushes and gears.

The pitching range of a turbine blades is typically from 0 to 90° however during normal power production the pitch angle is likely to be 0–10° (depending on the blade profile and controller operation). The pitching of the blades is mainly to shed power and given the 'predictable' nature of the tidal flow resource a maximum pitching rate of 12°/second is deemed sufficient. As pitching occurs at the higher flow speeds, turbulence is much less of a problem than at lower flow speeds [24]. The choice of electric motor depends on several factors particularly the required speed (rpm), supplied voltage and torque generation. Designed with a maximum pitch rate of 12°/second (2 rpm), then the gearing system and motor must be sized accordingly. Typically motors with a supply voltage of 690 V (which would be the case if using a grid power supply) have a speed range of 1000–3000 rpm.

The electric motor selected in this work is the Siemens 1GG6 DC motor [27] which is a 10 kW machine with 1200 rpm. This requires a gearbox with an overall ratio of approximately 600:1. This is a relatively small gearbox with respect to gearboxes that operate between the high and low speed shafts of the turbine. A 2-stage planetary arrangement with the first stage gear ratio 20:1 and the second 30:1 is a plausible design. Established gearbox manufacturers Bonfiglioli produce such designs for use in the wind industry. The HDO series bevel gear unit [28] is within the pitch system design requirements for the notional tidal turbine in this work and is used henceforth.

2.3. Wind turbine pitch systems

Wind turbine pitch systems are similar in architecture to those employed in tidal turbines however the operating profiles are different. In a wind turbine, pitch systems are often used below rated power to mitigate the effects of turbulence in the air, as well as operating at rated power output. This means that the pitch system in a wind turbine is potentially in action much more frequently than for tidal turbines. Wind turbine pitch systems typically have 3 drive units to enable individual pitching of the blades. There are architectural differences and differences in the operating profiles between wind and tidal turbine pitch systems, however the components used are the same.

As there is currently no publicly available tidal turbine failure data, data from wind turbines is used in this research to provide a measure of comparison for the tidal turbine failure rate model. The wind turbine failure data comes from a variety of literature sources [7,29,30]. This data is averaged across several turbines and farms and is calculated under a constant failure rate assumption.

3. Failure rate model development

The probabilistic failure rate model for the electro-mechanical pitch system outlined previously is described in detail in this section. Each part of the pitch system is represented by a probabilistic physics-based failure equation. Each equation is a function of part specific design parameters.

3.1. Design parameter uncertainty

In this work, the COV is used as a measure of the uncertainty in the design parameter probability distributions. The COV shows the extent of variability in relation to the mean of the population. COV values are used to define levels of uncertainty in each design parameter allowing for turbine developers to select the appropriate level of uncertainty. The sources of uncertainty in the design parameters for a given component include: a lack of clarity or visibility on the specifics of the component design; uncertainty about the structure or applicability of the component design parameter equation; a lack of understanding about the loading conditions. Table 1 highlights the qualitative descriptors for each COV.

COV = 0.1 suggests the developer is confident about the design parameter in question. This may mean that the design specifics have been decided and that the physical phenomena modelled by the parameter does not have high levels of uncertainty. All design parameters have irreducible (aleatoric) uncertainties so the minimum uncertainty or highest confidence level is COV = 0.1.

COV = 0.2 suggests that the turbine developer may be somewhat uncertain about the component design specification or the expected loading profile. Design parameters which are directly related to tidal flow quantification are contenders for this level of uncertainty because there is a lot of uncertainty associated with tidal flow measurements [13].

Table 1
COV values and associated uncertainty levels.

COV = σ	Uncertainty Level
0.1	Low
0.2	Medium
0.3	High

COV = 0.3 suggests the turbine developer has very low confidence in the design parameter value and there is a large range of potential values, represented by a high uncertainty level. This represents a lack of confidence in the values for the parameter in question or a lack of understanding about the loading regime. Perhaps the design is not yet advanced to a stage where the parameter in question has been investigated thoroughly.

3.2. Dynamic seal

The failure rate λ_s for a Dynamic Seal [16] is highlighted in Equation (3).

$$\lambda_s = \lambda_{b,s} C_p C_q C_h C_f C_v C_t C_n C_{pv}, \quad (3)$$

$\lambda_{b,s}$ is the base failure rate, C_p is the fluid pressure influence factor, C_q is the leakage influence factor, C_{dl} is the seal diameter influence factor, C_h is the material hardness influence factor, C_p is the fluid pressure correction factor, C_f is the surface finish influence factor, C_v is the fluid viscosity influence factor, C_t is the temperature influence factor, C_n is the contaminant influence factor and C_{pv} is the influence factor for the pressure velocity (PV) parameter.

The fluid pressure influence factor is set to $C_p = 0.25$ because the fluid pressure difference between the sea water and inside the nacelle is less than 10 MPa (at 40 m water depth where the turbine is located the sea pressure is approximately 0.6 MPa). The allowable leakage factor $C_q = Q - 4.2$ where Q is the allowable leakage rate. Given the subsea location of the turbine, no leakage is permitted for the pitch system dynamic seals, therefore $C_q = 4.2$.

The material hardness influence factor $C_h = \left(\frac{\frac{E}{C}}{0.55}\right)^{4.3}$ where E is the Young's Modulus and C is the contact pressure. For the chosen seal design, the maximum operating pressure is 1 MPa. The Young's Modulus for a seal made of hard rubber composite is 0.7 MPa. Therefore $C_h = 2.82$.

The next influence factor is concerned with the surface finish of the seal. It is calculated as $C_f = 2^{\frac{f-10}{38}}$ where the surface finish (f) of the seal is in μin RMS. The surface finish for a dynamic seal f is typically between 10 and 20 μin RMS [31]. The midpoint of 15 μin is selected for this seal design. Therefore, $C_f = 1.1$.

The fluid viscosity factor C_v is conservatively estimated as 1 [16]. The temperature influence factor $C_t = \frac{1}{2^{\left(\frac{T_r - T_0}{18}\right)}}$ where T_r is the rated temperature of the seal and T_o is the operating temperature. T_o is assumed to never exceed 50 °C and T_r is conservatively assumed to be 60 °C (it is likely much higher than this). Therefore $C_t = 0.5$ which given the subsea nature of the turbine seems reasonable (temperature related reliability issues are unlikely given the turbine is naturally cooled by sea water).

The pressure velocity (PV) parameter influence factor $C_{pv} = \frac{PV_a}{PV_d}$ where PV_a is the actual PV factor during operation and PV_d is the designed PV factor. A conservative safety factor of 5 is assumed resulting in $C_{pv} = 0.2$. The contaminant influence factor C_n accounts for the effects of contaminants in contact with the seal. The seal is operating in a harsh subsea environment therefore this influence factor is likely to be high. In Ref. [32], $C_n = 3.5$. This value is used as the expected value of the GLN with a high uncertainty due to a lack of transparency in the origins of this value.

The base failure rate from Ref. [16] for a dynamic seal is 0.2 failures/year of continuous operation. Based on a targeted 99% availability and with the pitch system unit operating around 33% of the time, $\lambda_{b,s} = 0.065$ failures/yr. The base failure rate for a seal from another prominent study into wave energy converter reliabilities [33] uses 0.036 failures/year for the failure rate of the seal. The largest of these values is employed in this work, $\lambda_{b,s} = 0.065$ failures/yr.

The essential dynamic seal design parameters that affect the failure rate are the surface finish f of the seal, the Young's Modulus Y, the contact pressure C, the rated temperature Tr and operating temperature To (see Table 2).

3.3. Roller bearing unit

The failure rate λ_b for a roller bearing [16] is highlighted in Equation (4).

$$\lambda_b = \lambda_{b,b} C_r C_v C_{cw} C_t C_{sf} C_c \quad (4)$$

$\lambda_{b,b}$ is the base failure rate. $\lambda_{b,b} = 1/\frac{L_s}{L_a}^{3.3}$ where L_s is the dynamic load rating of the bearing and L_a is the equivalent radial load. The dynamic load rating is found in the manufacturers data sheet and the equivalent load can be estimated from turbine simulations. In later stages of turbine development detailed simulations can be performed to understand the fluctuating loading on the bearing, however at the early design stage this is unfeasible for developers to undertake. In the absence of manufacturers base failure rate data, a relevant value is selected from the literature. Assuming a design safety factor of 1.2 for the bearing, then $\lambda_{b,b} = 0.55$ failures/million hours of operation [25]. With the pitch system operating 33% of the time and a targeted 99% availability, this results in $\lambda_{b,b} = 0.00157$ failures/yr. In the tidal turbine reliability study of a drive train main bearing in Ref. [3], values of $\lambda_{b,b} = 0.0137$ and $\lambda_{b,b} = 0.0694$ are employed. This drive train bearing is much larger than the pitch system application here. In Ref. [33] more generic tidal turbine bearing failure rate data is presented, ranging from $\lambda_{b,b} = 0.002$ to $\lambda_{b,b} = 0.02$.

The life adjustment factor C_r represents the probability of failure of the bearing; at a 10% level of failure probability $C_r = 1$. Lowering the acceptance level results in an increase in this value however a 10% probability of failure is typical when designing bearing units [34].

The lubrication deviation influence factor $C_v = \left[\left(\frac{V_1}{V_0}\right)^{0.54}\right]$ with V_o the actual operating viscosity of the lubricant and V_l the rated viscosity. $V_1 = 45000 n^{-0.83}(0.5(d + d_1)^{-0.5}$ where n is the oscillations per minute (opm) of the bearing. For an external bearing diameter $d_1 = 850$ mm and internal bearing diameter $d = 750$ mm and under the conservative assumption that n cannot exceed 2 rpm (which equates to one full oscillation every second), $V_1 = 31$ mm^2/s. The viscosity ratio $k = \frac{v_0}{v_1}$ and must be in the range 1–4 [25]. The actual operating viscosity V_0 is determined by the operating temperature of the bearing and the ISO viscosity grade (VG) of the lubricant [35]. Assuming that the bearing temperature does not exceed 50 °C (which is highly conservative given that the seawater temperature is considerable lower than this) with a ISO VG 220 lubricant then the operating viscosity $V_0 = 100$ mm^2/s [36]. This results in a viscosity ratio $k = 3.16$ which satisfies the range condition. Therefore, $C_v = 0.53$.

The lubricant contaminant factor $C_{cw} = 1.176(0.21^{0.01-CW})(FR)^{0.25}$ where FR is the oil filter rating in μm and CW is the percentage of water content in the lubricant. FR is assumed to be 20 μm [3]. The worst case scenario for water content in turbine lubrication oil (CW) is considered to be 0.1% [37]. Varying CW between 0.01 and 0.1% has a negligible impact on the value of C_{cw} therefore the upper limit 0.1% is chosen. This

Table 2
Dynamic Seal influence factor expected values and coefficient of variation (COV).

Influence Factor	Name	Expected Value = $\boldsymbol{m}$	COV = $\boldsymbol{\sigma}$	Associated design parameters
C_p	Fluid pressure	0.25	Low	–
C_q	Leakage	4.2	Low	–
C_h	Hardness	2.82	Low	Y, C
C_f	Surface finish	1.1	Low	f
C_v	Viscosity	1	Low	–
C_t	Temperature	0.5	Low	T_r, T_0
C_n	Contaminants	3.5	High	–
C_{pv}	Pressure velocity	0.2	Low	PV_d
$\lambda_{b,s}$	Base failure rate	0.048	Medium	–

results in $C_{cw} = 2.49$.

The operating temperature influence factor $C_t = 1$ as the operating temperature of the bearing is not anticipated to exceed 100°C [16]. The contamination influence factor $C_c = 1$ because the bearing is assumed to at least initially have extreme levels of cleanliness.

C_{sf} is the operating service condition influence factor and is determined by the loading regime on the bearing. A uniform and steady load would result in $C_{sf} = 1$ however given that the tidal turbine operates in a turbulent flow environment, the value of this factor is increased to 1.3 which is equivalent to a 'moderate shock load' application type [16]. This parameter is deemed to have a high level of uncertainty because of the difficulty in accurately quantifying turbulence metrics [13]. Table 3 demonstrates the roller bearing influence factor values.

3.4. Gearbox

The failure rate for a gear [16] is highlighted in Equation (5).

$$\lambda_g = \lambda_{b,g} C_{gs} C_{gp} C_{ga} C_{gl} C_{gt} C_{gv} \tag{5}$$

$\lambda_{b,g}$ is the gear base failure rate in failures per million hours of operation. The base failure rate ideally would be obtained from the component manufacturer. However, this often is proprietary information so it can be necessary to use generic failure rate data. The recommendation as per [16] is 1 failure per every 100 million gear revolutions. Gearbox failure rate data collated from a variety of relevant sources can be found in Refs. [33]. The failures per year of a generic drive train based gearbox used in offshore energy applications are 0.09–1.04 failures/yr. As the pitch system gearbox in this application is smaller than a typical gearbox on the turbine main shaft, a value of $\lambda_{b,g} = 0.2$ failures/yr is selected for the expected value of the GLN (COV is selected as medium).

$C_{gs} = \left[1 + \left(\frac{Vop}{Vd}\right)^{0.7}\right]$ which is the influence factor for speed deviation with Vo representing the operating speed and Vd representing the design speed. If designed correctly, then $Vo < Vd$. To be conservative it is assumed that $Vo = Vd$ therefore $C_{gs} = 1.62$ (which is considered a high estimate).

$C_{gp} = \left[\left(\frac{Lo/Ld}{0.5}\right)^{4.69}\right]$ which is the influence factor for loading with Lo representing the operating load and Ld representing the design load. The gearbox is typically designed to withstand extreme loads that are determined via simulation of the tidal flow environment. Given the uncertain nature of quantifying the tidal flow environment C_{gp} is decided to have a medium COV. The extreme designed for load is anticipated to be 50% higher than the typical operating load experienced by the turbine. This results in $C_{gp} = 1$.

$C_{ga} = [12.44(A_e)^{2.36}]$which is the influence factor for gear misalignment with A_e representing the misalignment angle in degrees. For a small gearbox, such as the one in the pitch system unit, provided it is well designed, $A_e < 0.5°$. Therefore, a conservative estimate of $C_{ga} = 2.42$.

$C_v = \left[\left(\frac{V_i}{V_o}\right)^{0.54}\right]$ which is the influence factor for lubrication deviation. The lubrication system for the bearing and gearbox is the same therefore $C_{gl} = 0.53$ as it was for the bearing unit. The influence factor for temperature $C_{gt} = 1$ as the gears are anticipated to not exceed 71°C. The influence factor for servicing $C_{gv} = 1.25$ which represents a 'medium shock' load. This is representative of turbulent tidal flow conditions acting on the driven member (i.e. the turbine blades and bearing unit). Table 4 demonstrates the gearbox influence factor values.

3.5. Electric motor

The failure rate λ_m for an electric motor [16] is highlighted in Equation (6).

$$\lambda_m = \left(\lambda_{b,m} C_{sf}\right) + \lambda_{wi} + \lambda_{bs} + \lambda_{st} + \lambda_{as} \tag{6}$$

$\lambda_{b,m}$ is the base failure rate for the electric motor. For a DC motor $\lambda_{b,m} = 2$ failures per million hours of operation [16]. C_{sf} is the motor load service factor. For a 'medium impact' loading regime which represents the bidirectional and reversible operation of a motor $C_{sf} = 2$. Given that this factor is directly related to the loading regime and associated uncertainties the COV for this factor is medium.

Table 3
Roller bearing unit influence factor expected values and coefficient of variation (COV).

Influence Factor	Name	Expected Value = $\boldsymbol{m}$	COV = $\boldsymbol{\sigma}$	Associated design parameters
C_r	Life	1	Low	–
C_v	Lubrication deviation	0.43	Low	V_1, V_0, d_1, d, n
C_{cw}	Lubricant contaminants	2.86	Low	FR, CW
C_t	Temperature	1	Low	–
C_{sf}	Service	1.3	High	Loading
C_c	Contaminants	1	Low	–
$\lambda_{b,b}$	Base failure rate	0.02	High	Loading

Table 4
Pitch system gearbox influence factor expected values and coefficient of variation (COV).

Influence Factor	Name	Expected Value = $\boldsymbol{m}$	COV = $\boldsymbol{\sigma}$	Associated design parameters
C_{gs}	Speed	1.61	Low	V_{op}, V_d
C_{gp}	Loading	1	Medium	L_o, L_d
C_{ga}	Gear angle	0.73	Low	A_e
C_v	Lubrication	0.53	Low	V_l, V_o
C_{gt}	Temperature	1	Low	–
C_{gv}	Service	1	Low	–
$\lambda_{b,g}$	Base failure rate	0.2	Medium	–

$\lambda_{wi} = \lambda_{wi,b} C_t C_v C_{alt}$ which is the failure rate of electric motor windings where $C_t = 2^{(T-40)/10}$ and T is the ambient temperature surrounding the motor at full load operation. T has previously been defined conservatively as 50 °C therefore $C_t = 2$. $C_v = 2^{(10Vd)}$ where Vd is the voltage tolerance of the motor (the ratio of operating to rated voltage). The maximum allowable voltage variation for a small DC motor (<1 kV) is 20% as per the requirements of British Standard 60034–1:2010 [38]. Using $Vd = 10\%$ results in $C_v = 2$. C_{alt} is the altitude influence factor and as the turbine is operating subsea altitude considerations are not relevant therefore $C_{alt} = 1$. $\lambda_{wi,b}$ is the base failure rate of the motor windings which can be provided by the manufacturer. However, if this information is not available a value of $\lambda_{wi,b} = 40$ failures per million hours can be used. $\lambda_{wi} = 320$ failures per million hours of operation.

λ_{bs} is the failure rate of the motor brushes. According to Ref. [5,16], $\lambda_{bs} = 3.2$ failures per million hours. λ_{st} is the failure rate of the stator housing. According to Ref. [5] $\lambda_{st} = 0.001$ failures per million hours.

λ_{as} is the failure rate of the armature shaft. $\lambda_{as} = \lambda_{b,as} C_f C_t C_{dy} C_{sc}$ where the base failure rate for the armature shaft $\lambda_{b,as} = 0.0061$ failures per year [33]. C_f is the surface finish influence factor and for a polished finish shaft $C_f = 1$. $C_{dy} = 1$ which is the shaft displacement influence factor. $C_{sc} = 1$ which is the stress concentration factor. Table 5 demonstrates the motor influence factor values.

The motor failure rate formula in Equation (6) assumes continuous motor operation. However, the pitch system only operates at rated flow velocity. Equation (7) calculates the corrected failure rate with h representing the percentage of time the turbine spends at rated velocity.

$$\lambda_{em} = \lambda_m * h \tag{7}$$

3.6. Numerical framework

The individual component failure rate probability density functions are then combined into one distribution representing the entire pitch system. The complete pitch system consists of three bearings, three seals, one gearbox and one electric motor as highlighted in Fig. 3. A Monte Carlo approach was developed to generate draws from each of the component distributions. Given that each pitch system component is fully described by a Generalized LogNormal distribution, samples can be randomly drawn and then summed together as per the RBD formulation in Equation (2). The authors used 100,000 samples to approximate the probability density function of the complete pitch system. A Generalized LogNormal distribution was then fit to the samples (details of the fit statistics can be found in Table 6 in the next section). Fig. 4 highlights the convergence of the Kolmogorov Smirnov test statistic (D) with an increasing number of simulations. As the value of D approaches zero, the fitted distribution approximates the real distribution increasingly accurately. The authors selected 100,000 simulations ($D = 0.0024$) as an acceptable cut off point to reduce computation time. For reference, the simulations were carried out using Python and took approximately 30 min to run using an Intel i5-5300U CPU with a clock speed of 2.3 GHz and 8 GB RAM.

4. Results

The individual component failure rates for the pitch system components are shown in Fig. 5. The electric motor has the largest mean failure rate; the bearing unit has the smallest. The confidence levels for the bearing and seal are higher than for the electric motor and gearbox.

The distribution for the complete pitch system is highlighted in Fig. 6. The mean value for the distribution is 0.627 failures per year with a 95% confidence interval of 0.482–0.811.

The reliability function for the complete pitch system consisting of three bearings, three seals, a gearbox and electric motor is highlighted in Fig. 7, with 95% confidence levels. A 50% probability of failure for the entire pitch system occurs between 0.9 and 1.5yrs. Also highlighted is the reliability function using base failure rates

Table 6
Component and combined pitch system GLN fit statistics.

Component	Expected value	95% Confidence Limits	p-value
Seal	0.062	0.025–0.128	0.24
Bearing	0.045	0.016–0.102	0.44
Gearbox	0.133	0.061–0.252	0.55
Electric Motor	0.174	0.123–0.242	0.43
Pitch System Total	0.627	0.482–0.810	0.35

Table 5
Electric motor influence factor expected values and coefficient of variation (COV).

Influence Factor	Name	Expected Value = $\boldsymbol{m}$	Units	COV = $\boldsymbol{\sigma}$	Associated design parameters
C_{sf}	Loading	2	–	Medium	h
λ_{wi}	Winding failure rate	0.149	Failures/year	Medium	V_d, T, h
λ_{bs}	Brush failure rate	0.008	Failures/year	Low	h
λ_{st}	Housing failure rate	0.000003	Failures/year	Low	h
λ_{as}	Shaft failure rate	0.000016	Failures/year	Low	h
$\lambda_{b,m}$	Base failure rate	0.026	Failures/year	Low	h
h	Rated operating time	33	%	–	–

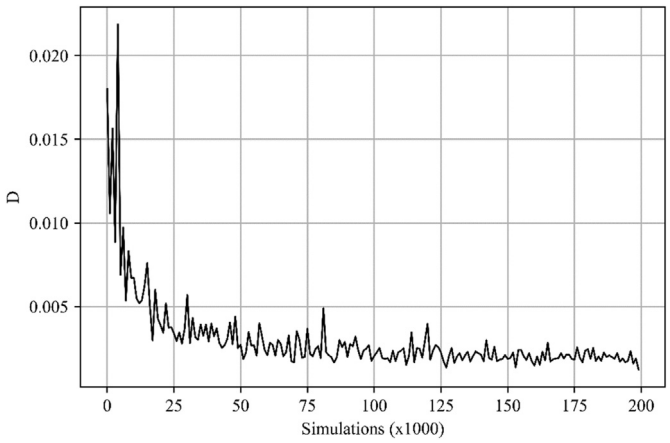

Fig. 4. Convergence of the Kolmogorov Smirnov statistic (D) with increasing number of simulations.

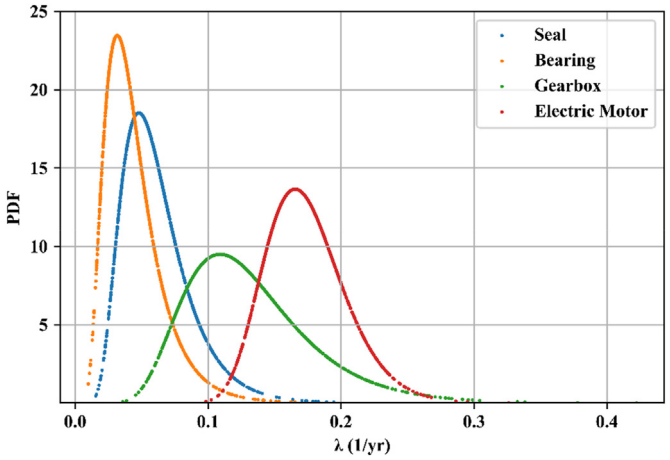

Fig. 5. Generalized Log Normal failure rate distributions for tidal turbine pitch system components: Dynamic Seal (blue), Roller Bearing unit (orange), Gearbox (green) and Electric Motor (red).

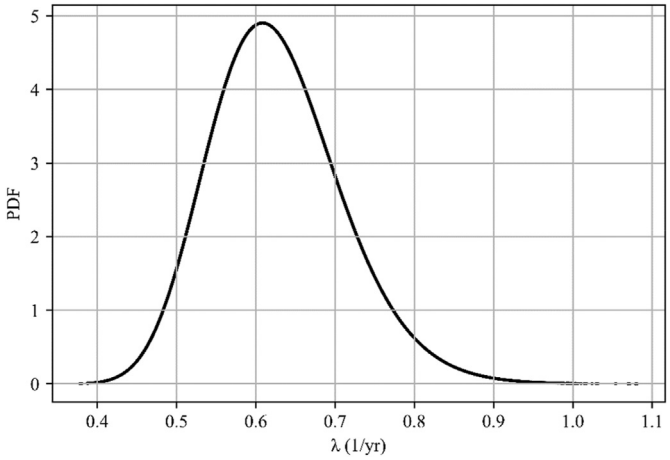

Fig. 6. Generalized Log Normal failure rate distribution for complete pitch system constituting 3xDynamic Seal, 3xRoller Bearing unit, 1xGearbox and 1xElectric Motor.

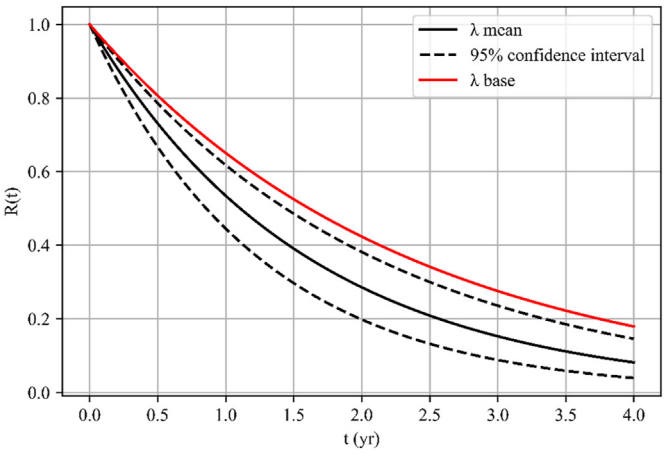

Fig. 7. Exponential reliability function for complete pitch system unit using mean failure rates (solid line) with 95% confidence levels (dashed line) and using uncorrected failure rates (red line).

(i.e. uncorrected failure rates). The reliability of the pitch system unit is therefore reduced as a result of applying the correction factors. This is to be expected because the base failure rates are generic and do not consider the anticipated loading conditions.

Table 6 displays the fit statistics for each of the pitch system components. The one-sample Kolmogorov Smirnov test is used to test the null hypothesis that the fitted distribution is Log Normal. P-values significantly greater than 0.05 suggest that the null hypothesis cannot be rejected. For each of the components the distribution fit is acceptable.

4.1. Comparison with wind turbines

Given the scarcity of tidal turbine failure data, the tidal turbine pitch system failure rate model cannot be validated with operational data. However, it can be compared in relation to wind turbine failures found from relevant literature. Table 7 lists pitch system failure rate data from a range of sources, encompassing both onshore and offshore turbines with both Electro-mechanical and Hydraulic designs. The wind turbine results listed are all average failure rates from several turbines. Data for offshore turbines with electric pitch systems are currently unavailable.

One of the difficulties in comparing failure data from various failure databases is the lack of consistency in the definition of failure. The highest failure rate in Table 7 is from the Chinese CWEA database [40]. This dataset has no failure definition and data is included from turbine commissioning, therefore it is likely to include early 'burn-in' failures that inflate the failure rate value. There is little information about turbine ratings although 1.5–6 MW is given as an indicative range. The second highest failure rate comes from offshore turbine data from Ref. [39]; no information about turbine rating or pitch system type is provided however given the turbines are offshore it is reasonable to assume that they are multi-MW devices. This data is also the most recent. The next highest failure rate comes from Ref. [7] which is also a study on offshore turbines, these devices all have a hydraulic pitch system and are rated between 2 and 4 MW. Failure is defined as a visit to a turbine outside of a scheduled operation. The final two failure rates come from Refs. [41,42]. These studies analyze turbine failures from the Landwirtschaftskammer (LWK) dataset. The failure rate from Ref. [41] is from a set of direct drive 0.5 MW turbines and the failure rate from Ref. [42] is from a set of 1.5 MW and

Table 7
Wind turbine and tidal turbine pitch system failure rates.

Turbine rating (MW)	PS type	Location	Country	Period	Number of Turbines	Failure rate (1/yr)	Source
2–4	Hydraulic	Offshore	U.K	2008–12	~350	1.076	[7]
?	?	Offshore	U.K	2015–16	1045	1.397	[39]
1.5–6	Electric	Onshore	China	2010–12	111–640	1.558	[40]
0.5	Electric	Onshore	Germany	1998–05	10–75	0.3	[41]
1.5, 1.8	Electric	Onshore	Germany	1998–05	3–22	0.45	[42]
1.5	Electric	Tidal	–	–	–	0.627	–

1.8 MW turbines. In both datasets, the pitch systems are electrical. The average failure rate of all the wind turbines in Table 7 is 0.956 failures/year; this is approximately 50% higher than the value from the tidal turbine failure rate model. This is partly because of the high failure rates from the Chinese data set skewing the results via a definition of failure that is not as strict as the European data sets. Also, the turbines in this data set have higher ratings than the tidal turbine model.

5. Sensitivity analysis

The effect of the independent design variables on component failure rates is assessed via an X–Y sensitivity analysis [43]. Each variable is held constant whilst one is varied over an allowable range (determined by engineering principles for each parameter). The sensitivity analysis helps to determine the relationship between each of the design parameters and the overall component failure rate.

Fig. 8 shows the Dynamic Seal and Roller Bearing failure rate sensitivities for each of their respective underlying design parameters. The base failure rate for each component is a key driver of the overall failure rate; this is represented by the steep gradient for λ_{base} in Fig. 8(a) and (b). The steep gradient of the E/C ratio (Young's Modulus/Contact Pressure) for the Dynamic Seal in Fig. 8(a) is also apparent. Extremely large values for this ratio would likely be a result of a mismatched design.

Fig. 9 shows the sensitivity of the Gearbox and electric motor failure rates to variations in their respective underlying design parameters. It can be seen in Fig. 9(a) that the steepest gradient line is associated with the gear misalignment parameter A_e. Small increases in gear misalignment have a large impact on the gearbox failure rate. This data is not normalized therefore misalignment values can be read directly from the graph; values greater than approximately 0.4° result in a sharp increase in the failure rate. In Fig. 9(b) the sensitive design parameters are the voltage tolerance level of the electric motor and the amount of operating time. The voltage tolerance level V_d must be kept within its boundaries else the failure rate can be adversely affected. All of the design parameters for the Electric Motor are influenced by the operating time/profile of the pitch system. Increases in the motor operating time result in linear increases in the motor failure rate. The amount of operating time of the motor is directly governed by the overall turbine design philosophy, control regime and site specific flow conditions; an understanding of these alongside the critical design parameters for each component of the pitch system is crucial for early stage tidal turbine developers to make informed design choices.

6. Discussion

The probabilistic failure rate model developed in this research has employed a physics-based approach. Given the lack of available failure data for tidal turbines, statistical assessments of operational data (as is common in the wind industry) are not viable. The physics-based approach has advantages in that it enables links to be made between critical design parameters and failure rates, according to empirical Physics of Failure equations. This is important as it enables turbine developers to understand the failure critical parameters of their component designs. Many turbine developers do not have the capacity to perform costly accelerated life testing procedures, therefore they must determine in other ways that the equipment they purchase is fit for purpose. The approach outlined in this paper enables developers to gain some insight into the specifics of what drives component failures. The main limitations of this approach are that it requires detailed understanding of the component designs (which may not be available during the early stages of turbine development); it is also labor intensive as models are required for every part and component.

The critical design parameters effecting the failure rate and reliability for each component of a notional tidal turbine pitch

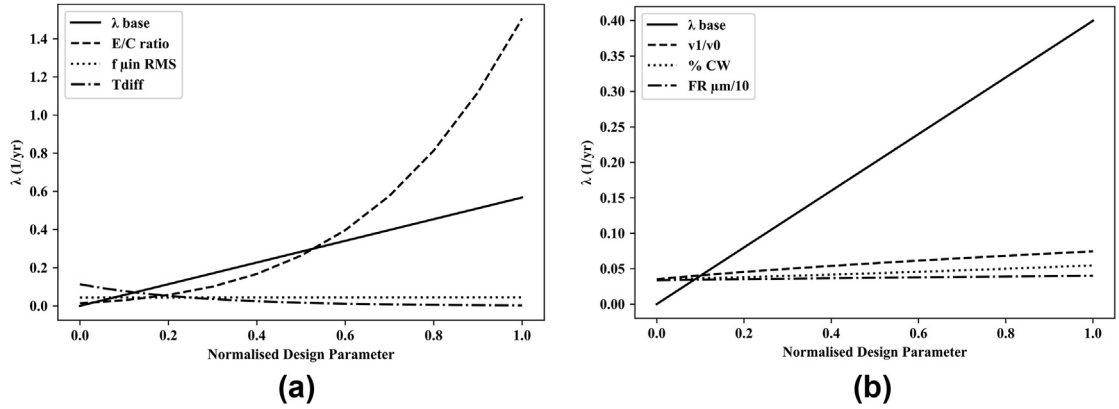

Fig. 8. X–Y Sensitivity analysis using independent feature-scaled design parameters (**a**) Dynamic seal failure rate sensitivity for normalized critical design parameters E/C ratio, f µin RMS, Tdiff and $\lambda_{b,s}$; (**b**) Roller bearing failure rate sensitivity for normalized critical design parameters V1/V0, %CW, FR µm and.$\lambda_{b,b}$

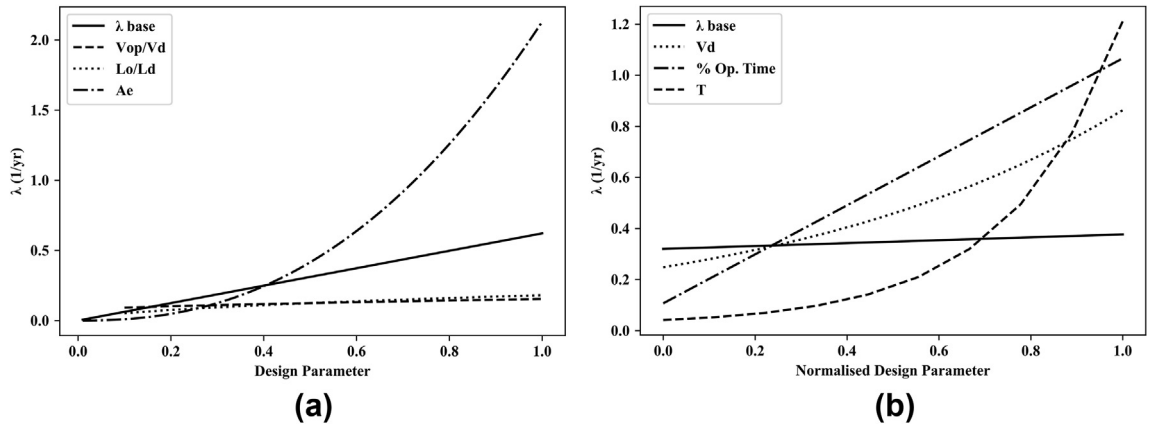

Fig. 9. X–Y Sensitivity analysis (**a**) Gearbox failure rate sensitivity for critical design parameters Vop/Vd, Lo/Ld, Ae and $\lambda_{b,g}$; (**b**) Electric motor failure sensitivity for normalized critical design parameters T, Vd, %Op. time and.$\lambda_{b,m}$

system have been outlined. The Dynamic Seal, which prevents water ingress into the turbine nacelle at the root of each blade, is highly sensitive to the E/C ratio (the ratio of the Young's Modulus of the seal material to its maximum operating pressure). The choice of material for the seal is crucial because even small increases in the E/C ratio can result in large increases in seal failure rate. A Young's Modulus of approximately 60% of the maximum seal contact pressure seems reasonable. The engineering tradeoff is that higher contact pressure ratings require stiffer seal materials with larger Young's Modulus values. Developers must be careful to assess the material properties of potential seal designs.

For the Roller bearing unit and Dynamic Seal the selection of a base failure rate is also crucial. These values should be available from the component manufacturer, however it is highly likely that the values from the manufacturer have been obtained from tests that are not specific to tidal turbine applications. As tidal developers often use 'off-the-shelf' components from the wind industry, this means that any component failure rate values must be treated with caution and corrected using the equations outlined in this paper.

For the gearbox, the gear misalignment angle is critical. Small levels of misalignment can cause wear and fatigue type failures. Given the exponential nature of the gear misalignment influence factor, it is advisable to ensure that the misalignment angle is below 0.5° (ideally as low a value as possible). Values larger than this result in rapid increases in the component failure rate. This value is design specific and developers need to ensure for their designs what the acceptable level of misalignment is.

The electric motor failure rate contributes the most to the overall pitch system failure rate. This is largely a result of the windings failure rate which dominates. This value is determined by the component manufacturer so it is imperative to select a manufacturer and design with a low winding failure rate. Temperature plays a key role in the winding failure rate therefore ensuring adequate cooling of the motor in the pitch system design is crucial. The Electric Motor voltage tolerance (ratio of operating to rated voltage) and operating time percentage are also critical design parameters. The voltage tolerance of the motor as per British Standard 60034–1:2010 should always be less than 20% (for a DC motor). Ideally the tolerance would be kept at a level much lower than this (somewhere in the region of 1% seems acceptable). The voltage tolerance depends on the power supply to the motor which could be from a battery or from the mains. Battery supply may provide a more stable voltage and also is protected against mains supply issues, however introducing a battery into the system means adding extra components which may adversely affect overall system reliability. One of the other key factors affecting the Electric Motor failure rate is the operating time. The operating time is linearly related to the failure rate. It is therefore important for developers to understand that the pitching regime design choice directly influences the failure rate of the electric motor. The amount of operating time of the pitch system is governed by the overall turbine design philosophy and rating, and also the control regime and site specific flow conditions. A trade-off exists between rating the turbine to extract more power from the tidal flow (i.e. spending more time at rated flow speeds), and the operating time and hence failure rate of the pitch system. This must be understood for each turbine design and site.

The largest failure rate uncertainties are associated with the gearbox and electric motor. For the motor this is because of uncertainty around the loading service factor and the winding base failure rate. For the gearbox, the uncertainties come from the loading factor and gear base failure rate. The loading factor contributes significantly to uncertainty in both the motor and gearbox which suggests that a detailed tidal flow measurement campaign at the proposed turbine location is required to accurately quantify the turbine loads and thus reduce model uncertainty.

In comparison with wind turbine pitch system failure rates found in literature, the pitch system design outlined in this research is approximately 50% lower than the average wind turbine pitch system failure rate. This is partly because of the larger ratings of the majority of the wind turbines (larger turbines have higher failure rates) and also because wind turbines pitch system operation is greater than tidal turbines, which typically only pitch their blades at rated flow speed. It is important for tidal developers to design for the lowest possible failure rates as the reliability requirements for tidal turbines are much higher than for wind turbines. Having a lower failure rate than wind turbines is likely not good enough; an order of magnitude lower could be the aim to ensure successful commercialization.

The physics-based failure relationships used in this research have been validated by the US Military (details of the experimental validation exercise can be found in Ref. [16]). The validation exercise was not conducted specifically with marine components, therefore the authors' stress the importance of dedicated marine component testing to determine the relevance of the empirical relationships. As more relevant failure data becomes available (e.g. pitch system component level failure data from the offshore wind industry), this can replace the generic base failure rates that are currently used in some of the component models. Beyond this, as

the tidal industry matures, pitch system failure data from operational turbines can be used to directly validate the failure rate predictions made using this approach. Comparisons between what the models predict and the reality of what occurs in the field can only take place once the industry has progressed to commercialization and failure reporting becomes commonplace (as happened in the early years of wind commercialization).

The probabilistic failure rate model developed in this research is anticipated to assist turbine developers, researchers and third party certifiers to model the failure rate of critical tidal turbine components. Using Physics of Failure principles and component design parameters enables a greater understanding of the design drivers of failure, which can aid the development of more reliable tidal turbines.

Funding

The support of the ETI and RCUK Energy Program funding for IDCORE (EP/J500847/1) is gratefully acknowledged. The second author would like to acknowledge the funding through the EPSRC Supergen ORE Hub [EP/S000747/1] and the Tidal Stream Industry Energizer Project (TIGER), a European Union INTERREG V A France (Channel) England Research and Innovation Program, which is co-financed by the European Regional Development Fund (ERDF).

CRediT authorship contribution statement

Fraser J. Ewing: Conceptualization, Methodology, Software, Formal analysis, Data curation, Writing - original draft, Writing - review & editing, Visualization. **Philipp R. Thies:** Methodology, Writing - review & editing, Supervision. **Jonathan Shek:** Writing - review & editing, Supervision. **Claudio Bittencourt Ferreira:** Funding acquisition, Supervision.

Declaration of competing interest

The authors declare that they have no known competing financial interests or personal relationships that could have appeared to influence the work reported in this paper.

References

[1] ETIP, Powering Homes Today , Powering Nations Tomorrow, 2019.
[2] MarineEnergyCouncil, UK Marine Energy 2019, 2019.
[3] Val, L. Chernin, Probabilistic evaluation of failure rates of mechanical components in tidal Stream turbines, in: EWTEC 2011 Proc., 2011.
[4] T. Delorm, Tidal Stream Devices : Reliability Prediction Models during Their Conceptual & Development Phases, 2014, p. 194.
[5] U.S. Department of Defense, Reliability Prediction of Electronic Equipment, 1991. Mil. Handb.
[6] P.R. Thies, G.H. Smith, L. Johanning, Addressing failure rate uncertainties of marine energy converters, Renew. Energy 44 (2012) 359–367.
[7] A. M, D.M. James Carroll, Failure rate, repair time and unscheduled O&M cost analysis of offshore wind turbines, Wind Energy 17 (April 2013) (2016) 657–669.
[8] Moog Industrial, Reliable Pitch Systems for a Lower LCoE, 2016.
[9] M. Wilkinson, B. Hendriks, F. Spinato, T. Van Delft, Measuring wind turbine reliability, results of the reliawind project, Eur. Wind Energy Assoc. Conf. (2011) 1–8.
[10] M. Rausand, A. Høyland, System Reliability Theory: Models, Statistical Methods, and Applications, 2004.
[11] P. O'Connor, Practical Reliability Engineering 45 (2) (2003).
[12] J. Wolfram, On assessing the reliability and availability of marine energy converters: the problems of a new Technology, Proc. Inst. Mech. Eng. Part O J. Risk Reliab. 220 (1) (2006) 55–68.
[13] D.R.J. Sutherland, Assessment of Mid-depth Arrays of Single Beam Acoustic Doppler Velocity Sensors to Characterise Tidal Energy Sites, 2015.
[14] B. Foucher, J. Boullié, B. Meslet, D. Das, A review of reliability prediction methods for electronic devices, Microelectron. Reliab. 42 (8) (2002) 1155–1162.
[15] J. McPherson, Reliability Physics & Engineering: Time to Failure Modelling, 2010.
[16] Naval Surface Warfare Centre, Handbook of Reliability Prediction Procedures for Mechanical Equipment, 2010.
[17] IRENA, "Tidal Energy:Technology Brief, 2014 no. June.
[18] DNV-GL, DNVGL-ST-0.164: Tidal Turbines, 2015, p. 230, no. October.
[19] S.T. Kandukuri, V.K. Huynh, H.R. Karimi, K.G. Robbersmyr, Fault diagnostics for electrically operated pitch systems in offshore wind turbines, J. Phys. Conf. Ser. 753 (5) (2016).
[20] Reproduced with permission from: J.G. Holierhoek, R.P. Van De Pieterman, H. Korterink, L.W.M.M. Rademakers, H. Braam, Setting up a prototype measurement campaign for mechanical components, in: Eur. Wind Energy Conf. Exhib. 2010, EWEC 2010, vol. 6, 2010, pp. 4767–4777. no. July.
[21] SIMEC Atlantis [Online]. Available: www.simecatlantis.com, 2019 https://simecatlantis.com/services/turbines/.
[22] NovaInnovation [Online]. Available: www.novainnovation.com, 2019 https://www.novainnovation.com/nova-m100.
[23] OrbitalMarinePower [Online]. Available: www.orbitalmarine.com, 2019 https://orbitalmarine.com/technology-development/the-concept.
[24] B. Sellar, G. Wakelam, Characterisation of tidal flows at the European marine energy centre in the absence of ocean waves, Energies 11 (1) (2018) 176.
[25] SKF, SKF rolling bearings catalogue. https://www.skf.com/binary/21-121486/Rolling-bearings–17000-EN.pdf, 2012.
[26] Wartsila, Seals, bearings & stern tubes catalogue. https://www.wartsila.com/docs/default-source/product-files/hydro-industrial/industrial-solutions-/seals-amp-bearings.pdf?sfvrsn=70f6f145_2, 2012.
[27] Siemens, DC motors catalog. https://cache.industry.siemens.com/dl/files/387/109763387/att_972109/v1/da12-2008-en.pdf, 2008.
[28] Bonfiglioli, Products range. https://www.bonfiglioli.com/international/usefulDocuments/br_cat_raind_std_eng_r01_0.pdf, 2019.
[29] J.B. Gayo, Final Publishable Summary of Results of Project ReliaWind, 2011.
[30] A.J. Carroll, A. Mcdonald, D. Mcmillan, Offshore Wind Turbine and Subassembly Failure Rates through Time, 2015.
[31] A.R. Products, Seal Design Guide, 2009.
[32] C. Iliev, Val, Tidal current turbine reliability : power take - off train models and evaluation, in: 3rd Int. Conf. Ocean Energy, 2010, pp. 1–6.
[33] P.R. Thies, Advancing Reliability Information for Wave Energy Converters, 2012.
[34] T.A. Harris, R.M. Barnsby, Life ratings for ball and roller bearings, Proc. Inst. Mech. Eng. Part J J. Eng. Tribol. 215 (6) (2001) 577–595.
[35] International Organization for Standardization, ISO 281:2007 Rolling Bearings - Dynamic Load Ratings and Rating Life, vol. 3, 2016 no. May.
[36] British Standards Institution, ISO 3448 Viscosity Grades of Industrial Liquid Lubricants, 1982.
[37] J. Zhu, J.M. Yoon, D. He, Y. Qu, E. Bechhoefer, Lubrication oil condition monitoring and remaining useful life prediction with particle filtering, Int. J. Prognostics Health Manag. 4 (2008) (2013) 1–15.
[38] British Standards Institution, BSI 60034-1:2010 Rotating Electrical Machines Part 1 : Rating and Performance, 2010.
[39] S. Pfaffel, S. Faulstich, K. Rohrig, Performance and reliability of wind turbines: a review, Energies 10 (11) (2017).
[40] Y. Lin, L. Tu, H. Liu, W. Li, Fault analysis of wind turbines in China, Renew. Sustain. Energy Rev. 55 (2016) 482–490.
[41] P.J. Tavner, G.J.W. Van Bussel, F. Spinato, Machine and converter reliabilities in wind turbines, Int. Conf. Power Electron. Mach. Drives (1) (2006) 1–4.
[42] F. Spinato, P.J. Tavner, G.J.W. Van Bussel, E. Koutoulakos, Reliability of wind turbine subassemblies, Renew. Power Gener. IET 1 (1) (2007) 10–16.
[43] B. Iooss and A. Saltelli, "Introduction : Sensitivity Analysis," pp. 1–26.